

## Movable and adjustable injection of air through concentrated sources of mass and momentum for the pneumatic atomization of polyurethane and the modeling of droplet-fiber-interaction for the manufacturing process of polyurethane-fiber-reinforced composites

P. Diffo<sup>\*</sup>, P. Wulf and M. Breuer

Department of Mechanical and Production Engineering, Hamburg University of Applied Sciences, Germany

[diffo@rzbt.haw-hamburg.de](mailto:diffo@rzbt.haw-hamburg.de), [wulf@rzbt.haw-hamburg.de](mailto:wulf@rzbt.haw-hamburg.de)

Department of Fluid Mechanics, Institute of Mechanics, Helmut-Schmidt-University Hamburg, Germany

[breuer@hsu-hh.de](mailto:breuer@hsu-hh.de)

### Abstract

For the manufacturing process of polyurethane-fiber-reinforced composites the liquid plastic polyurethane (PUR) is sprayed on a substrate. Simultaneously fibers are injected in the spray cone for wetting before the entire composite deposits and starts curing. The quantification of the influence of some process parameters like the air mass flow, the droplet size and distribution or the fiber injection angle on the fiber orientation and distribution on the substrate are to be analyzed. The modeling of the spray is carried out using a RANS Euler-Lagrange approach coupling the droplets with the gas phase in a four-way coupled manner. Thereby a new approach is presented for the moving air injection, where mass and momentum source terms are applied to a new set of adjacent cells according to the predefined motion of the injector. The fiber-droplet-coupling is realized either by artificially mixing the droplets and the air to a fictive fluid through a process called “homogenization” or by considering the dense droplet flow as an Eulerian phase through a process called “semi-homogenization”. The influences of both approaches are to be compared regarding the fiber distribution and orientation on a substrate.

### Introduction

The polyurethane spray molding process is a manufacturing technology applied to produce composites by spraying the initially liquid polyurethane (PUR) matrix together with reinforcing long fibers in a tool form or on a substrate. The fibers are laterally injected in the polyurethane-air spray cone for wetting before the entire composite is spread on the substrate, where it starts curing. In Figure 1 a PUR mixing head nozzle is shown together with the inclined fiber glass chopper on the left side. Mainly used in the sanitaryware industry for example to reinforce the rear-side of shower trays and bathtubs, this manufacturing process has found further applications in the agricultural machinery and utility vehicle sector and in the automotive industry. Especially in the latter sector the manufacturing of parts such as roof modules, cowls and fenders with nearly arbitrary shapes, resistance and stiffness require information about the average orientation and density distribution of fibers in the composite. This information is necessary for the prediction of the mechanical properties of the composite. Besides a study of the influence of process parameters (e.g., fiber injection angle, fiber mass flow, air and PUR mass flow and robot arm's speed during the processing) on the aforementioned distributions can be carried out. This study would make the process controllable, optimizable and the distributions predictable.

Therefore, in this paper an approach for the modeling and



Figure 1: Spray-fiber-injection manufacturing process [1]

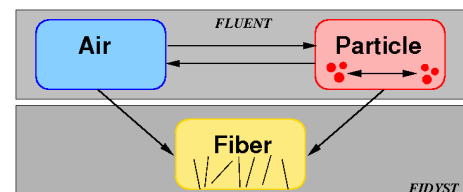


Figure 2: Multiple-way-coupling model

\* Corresponding author: [diffo@rzbt.haw-hamburg.de](mailto:diffo@rzbt.haw-hamburg.de)

simulation of the three phases (air, fibers and polyurethane droplets) within the spray jet and their different interactions (see Fig. 2) is considered. That includes the different impacts on the fiber distribution on the substrate. Different models for the fiber-droplet-coupling are considered and evaluated. A comparison with data from experiments carried out at the facilities of our industrial partner will be shown in a later publication. This paper focuses on the modeling of the gas phase using a new approach based on the utilization of source terms added to the transport equation of the gas phase. These source terms are applied to select control volumes (cells) of the computational domain to emulate the injection of air through a nozzle. The movement of the nozzle is virtually reproduced by adding the source terms only in the cells in which the nozzle is positioned. The novelty here is the aptitude to regulate the air jet cone angle and the air jet exit velocity independently from another. A second focus in this paper is placed on the coupling of the fibers with the droplets. Two approaches are thus presented called homogenization and semi-homogenization. Their impact on the fiber distributions will be analyzed.

### Simulation methodology

To model the whole process a sequential approach is undertaken (see Figure 3), where first a CFD simulation for the fluid and droplet phases is carried out followed by a fiber dynamics simulation. Within the CFD environment ANSYS FLUENT the modeling of the spray consisting of the gas-droplet mixture is performed using the built-in Euler-Lagrange approach for the tracking of the droplets in the continuous phase. The spray nozzle is not modeled as a solid body (wall + inlet) but as a point source (injector point in Figure 8), which can be moved through the computational domain with the help of User Defined Functions (UDFs). Thus we avoid the use of remeshing methods related to the movement of a body through a domain. The droplets generated are distributed near that point source according to predefined spray parameters [2]. The air jet is modeled by the activation of source terms in four adjacent cells (control volumes) which center points frame the moving point source. Thereby the exit velocity of the air jet is adjusted by increasing the momentum source until the expected velocity is reached. The source terms are the mass source term, representing the mass flow out of the nozzle and a momentum source term for each of the three momentum equations. Moreover, a transient RANS based, 4-way-coupled simulation is realized, during which specified data of each cell of the domain are exported for further use. These data are the density  $\rho$ , the velocity vector  $\mathbf{u}$ , the turbulent kinetic energy  $k$  and the turbulent dissipation rate  $\varepsilon$  of each phase (in case it exists), which are required in order to compute drag forces on each fiber within the subsequent simulation environment FiDyst. FiDyst stands for Fiber Dynamics Simulation Tool and computes the dynamics (displacement and deformation) of flexible fibers. It has been developed by the *Fraunhofer-Institute for Industrial Mathematics ITWM* (Kaiserslautern, Germany). To incorporate the presence of droplets, two approaches have been developed:

- the **homogenization approach**, which consists of computing a fictive density and velocity from the air and droplets information contained in each cell. Thus the cell seems to be filled with a fictitious, homogenized fluid called **H-fluid** (see Figures 4).
- the **semi-homogenization approach**, where separate data for the air and the droplets are exported. The droplets are “Eulerized” by computing a volume-fraction related, fictitious density and velocity in each cell which characterizes the semi-homogenized fluid (**SH-fluid**). Contrary to the aforementioned approach the gas and droplet phases are treated as two separated fluids which are applied to the fibers (see Figure 5).

These approaches enable a simple coupling of the droplets momentum with the fiber dynamics avoiding the direct calculation of the probability of local, highly stochastic collision events. Furthermore, the modeling of the explicit momentum transfer due to a collision of a droplet with a fiber is obsolete (see Figures 4 and 5).

To enable both types of simulations using either the H-fluid or SH-fluid preprocessors for geometry modeling and meshing of computational domains are used. For the computation of the fiber orientation and density distribution a MATLAB tool has been developed, which visualizes the fibers lying on the substrate and allows the retrieval of information about the distribution of selected areas on the substrate.

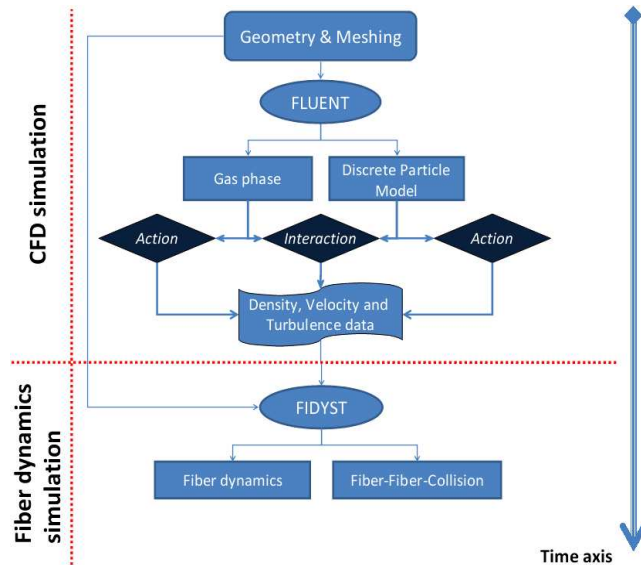


Figure 3: Workflow of a complete process simulation

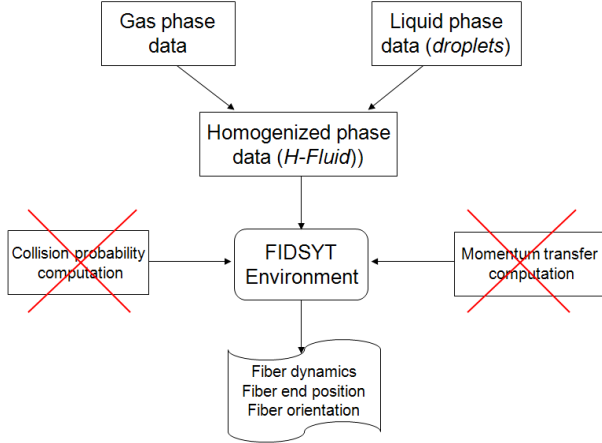


Figure 4: Homogenization approach for the fiber-droplet coupling

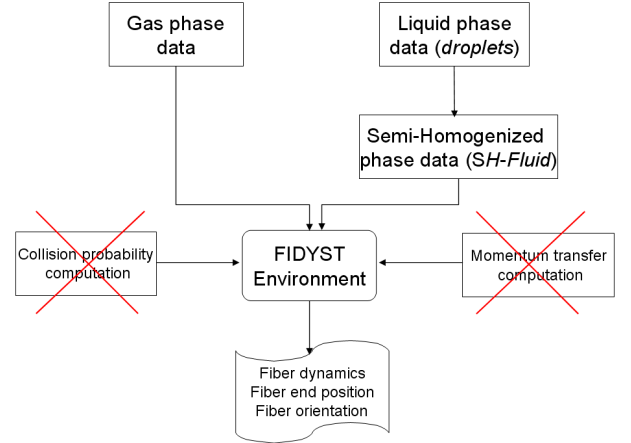


Figure 5: Semi-homogenization approach for the fiber-droplet coupling

### Modeling and simulation of the gas phase

An atomization process with the assistance of air leads to an accelerated disintegration of the liquid core in the primary stage of the disintegration. In the secondary stage a critical relative velocity between air and droplets leads to the break-up of droplets in smaller satellite droplets. A spectrum of smaller droplets is the result of this air-assisted atomization.

The governing equations for the gas phase are given in the Eulerian form based on the conservation equations for mass and momentum. For an incompressible fluid they read:

$$\rho \nabla \cdot \mathbf{u} = S_m \quad (1)$$

$$\rho \frac{\partial \mathbf{u}}{\partial t} + \rho (\mathbf{u} \cdot \nabla) \mathbf{u} = -\nabla p + \nabla \cdot \bar{\boldsymbol{\tau}} + \rho \mathbf{g} + \mathbf{F}_1 + \mathbf{F}_2 \quad (2)$$

The source term  $S_m$  refers to the mass added via UDF to the continuous phase by the injector.  $\mathbf{u}$  is the velocity vector,  $\rho$  the gas density,  $p$  the static pressure,  $\bar{\boldsymbol{\tau}}$  the stress tensor,  $\mathbf{g}$  the gravitational acceleration and the source term  $\mathbf{F}_1$  refers to external forces per unit volume that arise from the interaction with the disperse phase. This specific interaction source term is updated every iteration of the disperse phase equation and couples the gas flow with the liquid droplets.  $\mathbf{F}_2$  refers to the momentum source vector added via UDF to adjust the velocity vector in injector cells of the domain. Those cells are adjacent to the virtual injection point for droplets and are selected via an UDF.

Turbulence is taken into account by the Reynolds-Averaged approach using the realizable  $k$ - $\epsilon$ -model with  $k$  as the turbulence kinetic energy and  $\epsilon$  as the turbulence dissipation rate. Therefore, two transport equations for  $k$  and  $\epsilon$  are added to the precedent system of equations.

The addition of a control-volume specific mass source in the continuity equation (1) refers to the air mass flow out of the nozzle. It leads to a discharge  $S_m$  of air in all directions with a velocity inverse proportional to the area of the surfaces of the control volume (see Figure 6a). The subsequent addition of a momentum source term  $\mathbf{F}_2$  in equation (2) leads to the decay and bending of the velocity vectors in the directions different from the source term vector (see Figure 6b-c). This occurs in a transient simulation until the expected velocity vector is reached mimicking the final flow direction coming out of the nozzle (see Figure 6d).

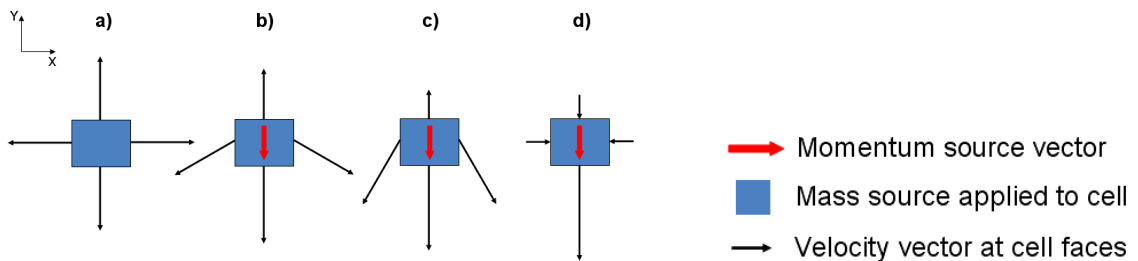


Figure 6: A single computational cell subjected to a) a mass source, b-d) a mass source and a downwards pointing momentum source vector

The magnitude of the vector components for the momentum source term  $\mathbf{F}_2$  is increased incrementally by a subroutine (UDF) in a closed loop until the velocity  $\mathbf{u}^i$  of the cell meets the required velocity  $\mathbf{u}_{\text{Goal}}$ . This subroutine, which functions like a controller, obeys the equation:

$$\mathbf{F}_2^{i+1} = \mathbf{F}_2^i + \lambda \cdot \Delta \mathbf{u} = \mathbf{F}_2^i + \lambda \cdot (\mathbf{u}_{\text{Goal}} - \mathbf{u}^i) \quad (3)$$

Hereby  $\lambda$  is the incremental factor, which converts the velocity difference into a force-like contribution and can be adjusted to accelerate the convergence of  $\mathbf{u}^i$  towards  $\mathbf{u}_{\text{Goal}}$ . The index  $i$  stands for the time-step while  $\mathbf{F}_2$  is the momentum source applied.

The modeling of a jet entering the domain from a nozzle with a hexahedral mesh using a single cell as the inlet region has shown poor results regarding the flow axisymmetry. Therefore, a study has been carried out which aims at the modeling of a movable, conical air jet with an adjustable cone angle and exit velocity through the simultaneous activation of many adjacent cells. To obtain the conical form of the air jet many constellations of neighboring cells (2-cells-, 3-cells- and 4-cells-models) have been tested regarding their delivery of an axisymmetric flow. Exemplarily, the 4-cells-models are presented in Figure 7. The next-to-last model with its four resulting vectors pointing away from each other has fulfilled the requirements best. The adjustment of the exit velocity follows the approach of equation (3) for each of the four cells.

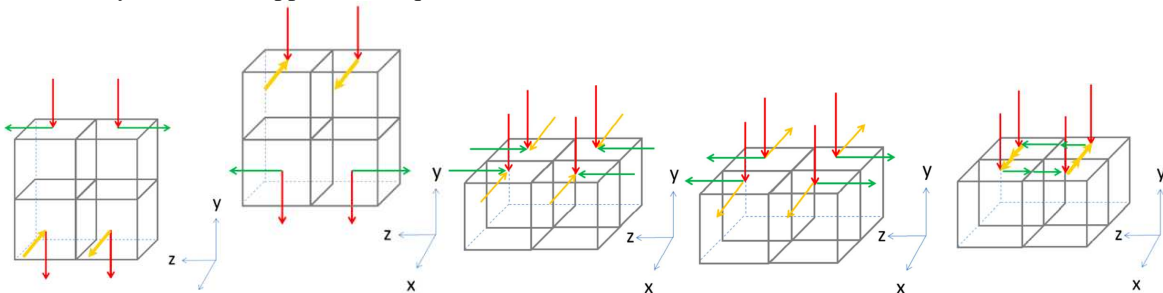


Figure 7: Different 4-cells-models tested for the modeling of an axisymmetric air jet

The motion of the virtual injector is operated through the activation of the appropriate four cells by a specific UDF. This UDF finds the cell in which the virtual injector is located (original cell A) and determines the four cells out of the neighboring cells (E, W, S, N, NE, NW, SE, SW), which center points frame the injector. Those four cells are marked as injector cells. The recognition process is done by dividing the original cell in four quadrants and by associating to each quadrant a combination of four neighboring cells. In Figure 8 the injector lies in quadrant 4. Therefore, the cell constellation (A, E, S, SE) is activated.

To each cell constellation the momentum source orientation vector for each cell can be likewise associated. By defining a cone angle the component of each vector can be computed so that they point away from each other according to the 4-cells-model.

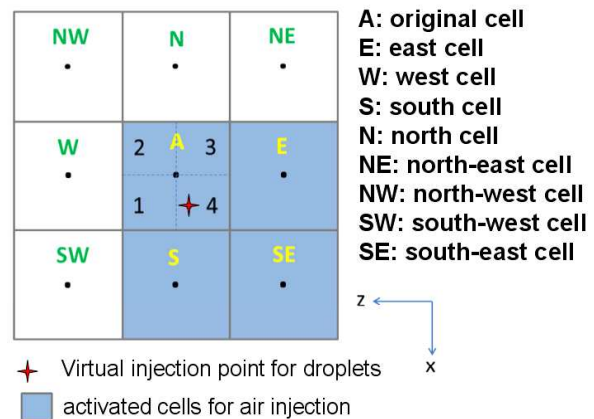


Figure 8: Example of a cell constellation for the virtual injector lying in quadrant 4 of the original cell (top view)

- The transient computation of the gas phase in the domain is performed with a pressure-based solver where:
- The time is implicitly discretized by a second-order accurate scheme (1e-04s timestep, 20 iterations/timestep).
  - The pressure is interpolated using the momentum equation coefficients (this is the standard approach in ANSYS-Fluent).
  - The pressure-velocity coupling is achieved by using the SIMPLE algorithm.
  - The spatial discretization of the convective terms of the different transport equations (momentum and turbulence) uses a second-order accurate upwind scheme.
  - The gradients are reconstructed at the cell faces according to the least-squares-cell based approach.
  - The air injected by the movable atomizer (1m/s velocity) is represented by two sources using UDFs. The air volume pouring into the domain is defined by a mass source ( $S_m$  in equation (1)), whereas three momentum sources account for accelerating the air up to the injector velocity ( $\mathbf{F}_2$  in equation (2)).
  - A third UDF determines the cell in which the atomizer presently resides. This information is needed for the origination of the liquid droplets.

### Modeling and simulation of the droplets

Since the disintegration process of the continuous fluid is highly complex, not completely understood and highly dependent on the nozzle geometry and on the presence of compressed air [3], in most CFD codes it is not part of the spray simulation. Instead the simulation starts with droplets injected from a virtual container into the domain according to a Rosin-Rammler-distribution. These droplets are then accelerated, deformed and shattered in smaller “satellite” droplets (liquid secondary atomization) by the co-flowing air.

To tackle the difficulty of computing simultaneously millions of particle trajectories and possible inter-particle collisions, the concept of “parcels” is used [4]. A parcel is a statistical representation of a number of individual droplets. It has the same properties as the represented particles and carries on top the number of represented particles as supplementary information. This reduction of the particle trajectories requires nonetheless submodels to balance the missing of particles in the coupling algorithms with the gas phase and with other particles (parcel-parcel-collisions).

The applied particle-particle collision model is based on the O’Rourke algorithm [5] which assumes that two parcels collide only if they reside in the same cell of the computational mesh during the present time step.

The governing equation for each parcel reads:

$$\frac{d\mathbf{u}_p}{dt} = f_D \cdot (\mathbf{u} - \mathbf{u}_p) + \mathbf{g} \frac{\rho_p - \rho}{\rho} + \mathbf{F}_3 \quad (4)$$

$\mathbf{u}_p$  and  $\rho_p$  are the velocity and the density of a spray droplet, respectively, while  $\mathbf{u}$  and  $\rho$  denote the velocity and the density of the gas phase.  $f_D \cdot (\mathbf{u} - \mathbf{u}_p)$  represents the drag force per unit mass with a dynamic drag model that accounts for the effects of droplet distortion by the assumption of a linear variation of the drag coefficient between that of a sphere and that of a disk [2].  $\mathbf{F}_3$  stands for all further external forces acting on the parcel during its motion. These are the “virtual mass” force from the acceleration of the fluid surrounding the particle, the additional force arising from the pressure gradient in the fluid generating a force on the particle due to different pressures acting on the particles surface and the Saffman’s lift force due to particle movement through shear flow. An additional force originates from the turbulence dispersion of particles. It is modeled by applying a stochastic tracking model (random walk) which uses stochastic methods to include the effects of instantaneous turbulent velocity fluctuations of the gas phase on the particles. This interaction of a parcel with a turbulent eddy, characterized by a Gaussian distributed random velocity fluctuation and the characteristic life time, prevail during the eddy life time. The secondary break-up of parcels is governed in this work by the Kelvin-Helmholtz-Rayleigh-Taylor (KHRT) model, which combines the effects of Kelvin-Helmholtz waves driven by aerodynamic forces with Rayleigh-Taylor instabilities due to the acceleration of shed droplets injected into freestream conditions [2].

The two-way coupling of air and particles is realized by the determination of momentum exchange between the gas phase and the parcels, according to the previously presented equations. When a parcel passes through a control volume of the computational mesh, the momentum transfer is initially computed by evaluating the momentum variation of the parcel in the present time step and adding a sink term to the gas phase momentum equation (2). The subsequent solution of equation (2) leads to a new gas velocity which is then reintroduced into the parcel momentum equation (5). This operation is repeated until convergence is achieved for both velocities.

The transient computation of the gas-liquid spray mixture in the domain is realized by the ANSYS Fluent built-in “solid cone model”. In brief, this is an injection point from which the gas and all the droplets or parcels, respectively, originate. The injection point can be moved in the domain during the computation to simulate a robot-driven path of the original PUR spray nozzle. The atomizer model requires:

- The number of parcels per injection time step,
- The time-dependent position vector for the injector,
- The relative velocity vector of the born parcels,
- The spray cone angle,
- The liquid mass flow rate,
- The nozzle diameter,
- The distribution function for the droplet diameters (here Rosin-Rammler-distribution),
- The diameter range of the droplets.

### Droplet-fiber-coupling

A newly developed approach for the coupling of the particles with fibers is presented. As already mentioned the apparent approach would be to detect individual collisions between the parcels and the fibers. This at a first glance apparent approach is, however, difficult to implement as the parcel concept makes it impossible to extract the exact position and momentum for each droplet. Furthermore, even if only the parcels would be accounted for,

the problem of collision detection and momentum transfer remains. To overcome this problem two approaches are presented.

(I) Both phases (gas and droplets) are averaged or “homogenized” to a new fluid, called “H-fluid” within the CFD environment (see Figure 4). The cell specific data ( $\rho_{cell}$ ,  $\mathbf{u}_{cell}$ ,  $k$  and  $\varepsilon$ ) of the new fluid are then used in the FIDYST environment to compute the dynamics of falling fibers. If  $\alpha$  is the volume fraction of droplets in a cell,  $\rho_{gas}$  and  $\rho_P$  are the densities of the air and the PUR-liquid, respectively, then the fictive density equals:

$$\rho_{cell} = \rho_{gas}(1 - \alpha) + \rho_P \alpha \quad (5)$$

The fictive velocity derives from the momentum conservation of both phases within a cell and reads:

$$\mathbf{u}_{cell}^{discrete} = \frac{\rho_{gas}(1 - \alpha)\mathbf{u} + \frac{\rho_P \sum_{i=1}^n N_i V_{p_i} \mathbf{u}_{p_i}}{V_{cell}}}{\rho_{cell}} \quad (6)$$

$\mathbf{u}_{p_i}$  is the velocity of a parcel  $i$  and  $N_i$  denotes the number of droplets within that parcel.  $n$  denotes the number of parcels within a cell.

(II) The droplets are merged to an Euler-fluid by computing a volume fraction related, fictitious density and velocities in each cell. The process is named “semi-homogenization” and the obtained fluid is called “SH-fluid”. Thus separate data for the air and the SH-fluid are exported. For the SH-fluid the equations governing the fictive density and velocities are:

$$\rho_{SH} = \rho_P \alpha \quad (7) \quad \text{and} \quad \mathbf{u}_{SH} = \frac{\sum_{i=1}^n N_i \mathbf{u}_{p_i}}{\sum_{i=1}^n N_i} \quad (8)$$

### Modeling and simulation of the fiber dynamics

First numerical simulations of single long fibers in a single flow were conducted at the beginning of the 90's with a particle simulation model which built the fibers as a chain of particles according to the beam-model [6]. Lately, the Fraunhofer-Institute for Industrial Mathematics ITWM has developed a simulation tool (FIDYST) to compute the dynamics of endless fibers for the melt-spinning process of nonwoven materials [7, 8].

To model long but finite fibers in a spray flow an adaption of the FIDYST software algorithm has been made. The trajectory and deformation of a fiber is based on the dynamical Kirchhoff-Love theory for the time-dependent behavior of a Cosserat rod (Cosserat continuum). This theory allows large, geometrically non-linear deformations [7]. Under the assumption of dominating elastic (extensile) effects, the Bernoulli-Euler material law is applied while considering a fiber as a one-dimensional inextensible elastic rod parameterized by its arc length  $s$  and time  $t$ . A single fiber can be specified mathematically by the balance of momentum and the preservation of the arc length:

$$\rho_F A_F \frac{\partial^2 \mathbf{r}}{\partial t^2} = \frac{\partial}{\partial s} \left( T \frac{\partial \mathbf{r}}{\partial t} \right) - E_F I \frac{\partial^4 \mathbf{r}}{\partial s^4} + \mathbf{f}^{grav} + \begin{cases} \mathbf{f}^{spray}(\mathbf{r}) + \mathbf{f}^{turb}(\mathbf{r}) \\ \mathbf{f}^{air}(\mathbf{r}) + \mathbf{f}^{droplet}(\mathbf{r}) + \mathbf{f}^{turb}(\mathbf{r}) \end{cases} \quad (9)$$

$$\left( \frac{\partial \mathbf{r}}{\partial s} \right)^2 = 1 \quad (10)$$

$\mathbf{r}(s,t)$  is the three-dimensional position of the fiber,  $T$  is a modified normal force,  $\rho_F$  is the fiber density,  $A_F$  is the fiber cross-section,  $E_F$  is the elasticity modulus,  $I$  is the momentum of inertia and  $\mathbf{f}^{grav}$  is the external gravitational force.  $\mathbf{f}^{spray}$  represents the fluid forces of the H-Fluid,  $\mathbf{f}^{air}$  the fluid force of the air and  $\mathbf{f}^{droplet}$  the force of the SH-fluid in the spray acting on the fiber. Similar to the splitting of the velocity in a mean and a fluctuating part as a result of the RANS approach, the external aerodynamic forces are separated into a deterministic mean force  $\mathbf{f}^{spray}$  of the spray or the air  $\mathbf{f}^{air}$ , respectively, and a stochastic turbulent force of the air itself  $\mathbf{f}^{turb}$ .

### Simulation set-up

A container (0.75m x 0.5m x 1.5m) is modeled and a hexahedral grid (75 x 50 x 150 cells) is generated (see Figure 9). The outcome is a mesh with a uniform cell volume of 1 cm<sup>3</sup> and a total number of 562,500 cells. The domain interior was initially filled with air and five of the six boundaries were defined as pressure outlets. Only the lower boundary in the XZ-plane is defined as a no-slip wall to represent the substrate with wall friction

for the gas phase and a trapping condition for the discrete droplets. The simulation consists of generating an air jet with a predefined cone angle and exit velocity and of moving the injection point with its parcels along a predefined path (see Figure 10). The subsequent fiber dynamics simulation is carried out along the same path with a fiber injection point following the spray injection point (see Figure 10).

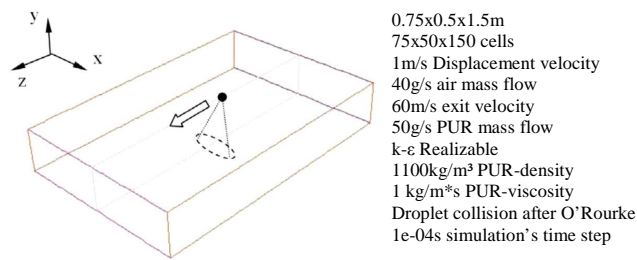


Figure 9: Computational domain with a spray cone, the moving direction of the injection point and some input data of the simulation depicted qualitatively

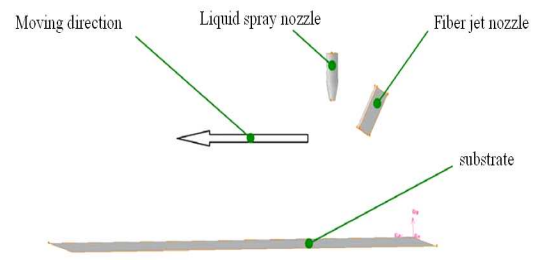


Figure 10: Fiber dynamics simulation with its geometry for the visualization and fiber-wall-contact

## Results

The velocity distribution at different heights along the injection axis depicted in Figure 11 shows an axisymmetric pattern of the flow. This is evident from the circular distributions of the velocity at the different heights considered. The decay of the velocity with increasing distance from the nozzle is also an important feature of free jets required for a correct prediction. That is observed in Figure 12A in theory (left) and in the simulation (right). Finally, the droplets transported by the air jet are depicted colored by their velocity in Figure 12B. As expected the high velocity droplets can be found near the air jet inlet cells and the stream of droplets shows a conical shape akin to the air jet shape in Figure 11.

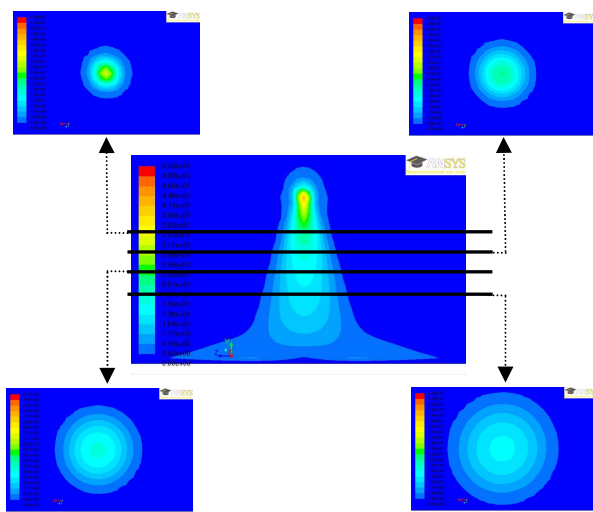


Figure 11: Velocity distribution in different planes orthogonal to the spray direction

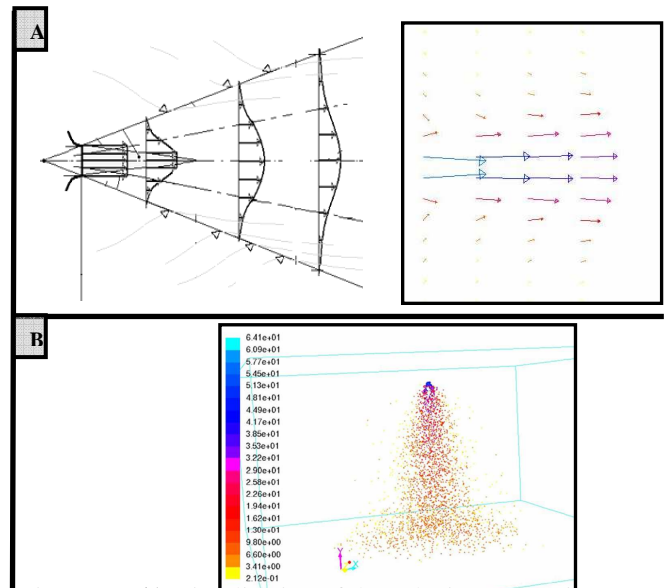


Figure 12: A) Visualization of the velocity vectors in the conical jet flow from theory [11] (left) and from the present simulation (right)

B) Visualization of the transported droplets colored by their velocity

The impact of the spray simulation on the fibers can be quantified by examining the distribution of the fiber on the substrate. Figure 13 shows an area of the simulated substrate with deposited fibers. A lattice is layed on the substrate and the fiber amount and orientation distribution per quadrant is plotted for both cases of homogenization and semi-homogenization (see Figure 14). For an accurate comparison the substrate area subjected to the analysis is restricted to a subdomain and used for both approaches of the spray impact.

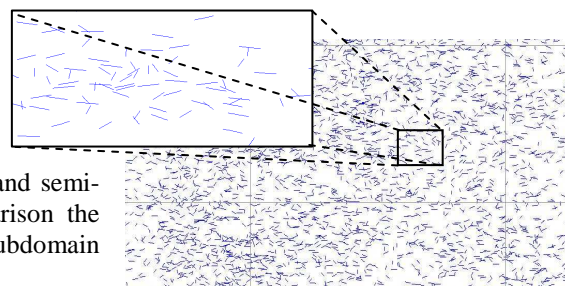


Figure 13: Substrate with deposited fibers

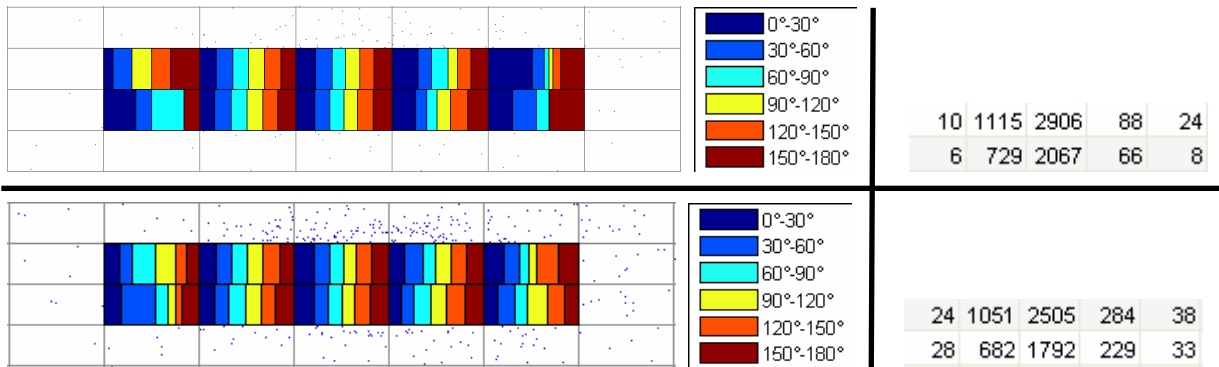


Figure 14: Orientation distribution of fibers on a subsurface of a substrate (left) with the related number of fibers per analyzed area (right) for the interaction of fibers with an homogenized spray (up) and a semi-homogenized spray (down)

First results are shown in Figure 14 where the middle region of the substrate (colored surface in Figure 14) represents the observed subdomain. The colored bars in each quadrant of the lattice signals the presence of fibers with the related orientation according to the legend. Furthermore, the length of these bars represents qualitatively the amount of fibers with the related orientation. The central quadrants of the lattice show almost a uniform orientation distribution in both approaches which vanishes in the corner quadrants. The number per surface area shows a non-uniform distribution and the numbers are different in every quadrant for both homogenization and semi-homogenization approaches. Noticeable is that the amount decreases rapidly in both cases in the direction of the corners with different gradients. This most likely occurs because the fiber injection begins and stops at those corners. Both approaches show a similar trend in the fiber orientation and number distribution.

### Summary and conclusions

A new approach is presented for the movement of an air injection in a spray process. For this purpose mass and momentum source terms are applied to a set of adjacent cells surrounding the virtual injector. It is even possible to add swirl to the injected air flow. We also presented two approaches to simplify the interaction modeling between fibers and droplets, the homogenization and the semi-homogenization approach. Regarding their impact on the distribution of fiber numbers and orientation both approaches show slightly different results. These results need to be validated by experiments. A more accurate model, which alternatively and more realistically determines the forces by estimating the probability of local collision events and modeling an extra force field related to the averaged momentum transfer per time step due to droplets collisions with a fiber is presently being developed. A complete comparison of these models with the experiments will be presented at the conference.

### Acknowledgements

The Johannes-Hübner-Stiftung Gießen is gratefully acknowledged for the financial support of this research.

### References

- [1] *Polyurethane – Composite Spray Moulding*, Advertising material of Hennecke GmbH, (2007).
- [2] *ANSYS Fluent User Guide*, Lebanon, (2010).
- [3] Lefebvre, A.H., *Atomization and Sprays*, Hemisphere Pub. Corp., (1989).
- [4] Paschedag, A.R., *CFD in der Verfahrenstechnik*, Wiley-VCH, (2004).
- [5] O'Rourke, P.J., *Collective Drop Effects on Vaporizing Liquid Sprays*, PhD thesis, Princeton University, (1981).
- [6] Yamamoto, S., Matsuoka, T., *Journal of Chemical Physics* 102: 2254-2261, (1995).
- [7] Hietel, D., *FIDYST – Fiber Dynamics Simulation Tool*, Innovation durch Simulationsunterstützung, oral presentation at the 23. Hofer Vliesstofftage, Hof, (2005).
- [8] Marheineke, N., *Turbulent Fibers - On the Motion of Long, Flexible Fibers in Turbulent Flows*, PhD thesis, Technische Universität Kaiserslautern, (2005).
- [9] Diffo, P., Wulf, P., and Breuer, M., *Int. Conf. on Multiphase Flow*, Tampa, Florida, May 30 - June 4, (2010).
- [10] Diffo, P., Wulf, P., Olawsky, F., Hietel, D. and Breuer, M., *The Int. J. of Multiphysics: Multiphysics Simulation - Advanced Methods for Industrial Engineering*, pp. 107-126, (2011).
- [11] N.N., *Modellierung turbulenter technischer Strömungen*, Lecture notes, Technical University Darmstadt (2011).